UpWind

Project funded by the European Commission under the 6th (EC) RTD Framework Programme (2002- 2006) within the framework of the specific research and technological development programme "Integrating and strengthening the European Research Area"

Project UpWind

Contract No.:
019945 (SES6)

"Integrated Wind Turbine Design"

COMPUTATIONAL DAMAGE MODEL OF FIBER REINFORCED COMPOSITES

AUTHOR:	Leon Mishnaevsky Jr.
AFFILIATION:	Forskningscenter Risoe, DTU
ADDRESS:	Frederiksborgvej 399, 4000 Roskilde Denmark
TEL.:	+45 4677 5729
EMAIL:	leon.mishnaevsky@risoe.dk
FURTHER AUTHORS:	Povl Brøndsted
REVIEWER:	Project members
APPROVER:	

Document Information

DOCUMENT TYPE	Deliverable
DOCUMENT NAME:	Computational model of damage initiation and growth in fiber reinforced composites
REVISION:	
REV.DATE:	
CLASSIFICATION:	R3: Restricted to WP3 members + PL
STATUS:	

Deliverable 3.2.1

Abstract: The investigations described in this technical report were performed in the frame of Task 3.2 “Micro-mechanics-based material model” of Work-Package WP3 “Rotor Structure and Materials” of the UPWIND project. Numerical micromechanical investigations of the mechanical behavior and damage evolution of glass fiber reinforced polymer matrix composites are presented. A program code for the automatic generation of 3D micromechanical unit cell models of composites with damageable elements is developed, and used in the numerical experiments. The effect of the statistical variability of fiber strengths, viscosity of the polymer matrix as well as the interaction between the damage processes in matrix, fibers and interface are investigated numerically. It is demonstrated that fibers with constant strength ensure higher strength of a composite at the pre-critical load, while the fibers with randomly distributed strengths lead to the higher strength of the composite at post-critical loads. In the case of randomly distributed fiber strengths, the damage growth in fibers seems to be almost independent from the crack length in matrix, while the influence of matrix cracks on the beginning of fiber cracking is clearly seen for the case of the constant fiber strength. Competition between the matrix cracking and interface debonding was observed in the simulations: in the areas with internsive interface cracking, both fiber fracture and the matrix cracking are delayed. Reversely, in the area, where a long matrix crack is formed, the fiber cracking does not lead to the interface damage. The conclusions of the computational analysis are compared with experimental data from literature.

Contents

<table>
<tr><th colspan="3">STATUS, CONFIDENTIALITY AND ACCESSIBILITY</th><th></th><th colspan="3"></th><th></th><th colspan="2"></th></tr>
<tr><th colspan="3">Status</th><th></th><th colspan="3">Confidentiality</th><th></th><th colspan="2">Accessibility</th></tr>
<tr><td>S0</td><td>Approved/Released</td><td></td><td></td><td>R0</td><td>General public</td><td></td><td></td><td>Private web site</td><td></td></tr>
<tr><td>S1</td><td>Reviewed</td><td></td><td></td><td>R1</td><td>Restricted to project members</td><td></td><td></td><td>Public web site</td><td></td></tr>
<tr><td>S2</td><td>Pending for review</td><td></td><td></td><td>R2</td><td>Restricted to European. Commission</td><td></td><td></td><td>Paper copy</td><td></td></tr>
<tr><td>S3</td><td>Draft for commends</td><td>x</td><td></td><td>R3</td><td>Restricted to WP members + PL</td><td>x</td><td></td><td></td><td></td></tr>
<tr><td>S4</td><td>Under preparation</td><td></td><td></td><td>R4</td><td>Restricted to Task members +WPL+PL</td><td></td><td></td><td></td><td></td></tr>
</table>

PL: *Project leader* **WPL:** *Work package leader* **TL:** *Task leader*

1. Introduction

Glass fiber-reinforced polymer (GFRP) composites are widely used in the low-weight constructions, due to the high strength of glass fibers, as well as due to the availability of efficient and low cost production technologies of the materials. Unidirectional composites with epoxy matrixes, which have better mechanical properties than the polyesters and vinyl resins, are often used in the aerospace and wind energy applications. The strength and damage resistance of composites can be predicted and ultimately improved if the effects of the properties of fiber, matrix and interfaces on the mechanical properties and strength of composites are known.

The purpose of this work is to develop computational tools for the numerical analysis of deformation and damage behavior of composites, and to analyze the damage mechanisms and the microstructure-strength relationships of glass fiber reinforced polymer matrix composites.

2. State-of-the art: Modelling of strength and damage of fiber reinforced composites

Several modeling approaches are traditionally used to simulate the damage and failure of fiber reinforced composites. Among them, one can differentiate the following main groups [1]:

- ***analytical models*** (often based on the shear lag model by Cox [2], and used to analyze the load transfer and multiple cracking in composites): e.g, break influence superposition (BIS) technique by Sastry and Phoenix [3], Green function model by Curtin and colleagues [4], etc.,
- ***fiber bundle model*** (FBM) developed initially by Daniels [5], and further improved and generalized by members of Herrmann' group at the University of Stuttgart, Germany [5-6],
- ***fracture mechanics-based models*** (often applied to the case of brittle matrix and fiber bridging, see the classical works by Marshall, Evans, Cox, Budiansky [7, 8], McCartney [9], etc.),
- ***continuum damage mechanics based models*** (Allen et al. [14], Hild and colleagues [11], etc.), and, finally,
- ***numerical continuum mechanical*** (often, finite element based) ***models*** [12-19, see also reviews 1, 20-21].

The analytical methods (shear lag based, LEFM based, and other analytical models, etc.) are applicable mainly to the linear elastic material behavior and relatively simple, periodic microgeometries. The generalization of these approaches to the non-linear material behavior, random and evolving microstructures and complex microgeometries can be rather difficult in many cases. In these cases, numerical versions of the analytical models, or continuum mechanical models solved by numerical discretization (finite element method, finite differences, etc.) are used. The advantage of the continuum mechanical models are that they do not include inherent basic assumptions, which may or may not hold for each new problem (as different from, e.g., shear lag based or fiber bundle based models). The continuum mechanical methods allow simple integration of the non-linear phase behavior, evolving microstructures, ideas of the continuum damage mechanics and fracture mechanics as well as probabilistic aspects of the composite behaviour.

Let us review some works on the ***continuum mechanical/numerical analysis*** of deformation and damage of unidirectional long fiber reinforced composites.

In a series of works [e.g., 12, 13]., the ***effect of the fiber arrangement on the deformation and overall behavior of composites*** was simulated using unit cell models with different (square edge-packing, diagonal-packing and triangle-packing [12], and clustered and even nonregular [13]) fiber arrangements. Babuška et al. [14] obtained a solution for the stress distribution in a 2D linear elastic problem with two fibers, using p-version of FEM. Then, they considered homogenization problem with hundreds of fibers, and obtained the stress distributions, histograms of the stress distribution and the relationships between effective stiffness coefficient and the volume fraction of fibers. Using unit cells with different fiber arrangements, Asp et al. [15] studied numerically the ***failure initiation*** (yielding and cavitation-induced brittle failure) and the effect of the interphases layer properties on the transverse failure in the polymer composites. Vejen and Pyrz [16] implemented the criteria of pure matrix cracking (strain density energy), fiber/matrix interface crack growth (bi-material model) and crack kinking out of a fiber/matrix interface into their own finite element package, and obtained numerically the ***crack paths for different fiber distributions***.

Sherwood and Quimby [17] modeled damage growth and the effect of the interface bonding strength in long fiber reinforced composites, using the non-linear time-dependent material model of the matrix. Considering several cases of the ***interface bonding*** (perfectly bonded interface, weakly bonded interface or completely debonded interface), they observed that the mechanical response of the composite with completely debonded interface is controlled by the mechanical behavior of the matrix, while the response of the cross-ply composite is controlled by the deformation and damage of fibers. Zhang et al. [18] studied toughening mechanisms of FRCs using a micromechanical model ("embedded reinforcement approach"), taking into account both fiber bridging and matrix cracking. They demonstrated that the strong interfaces can lead to the lower toughness of the composites. González and LLorca [19] developed a multiscale 3D FE model of fracture in FRCs, which incorporated three damage mechanisms (plastic deformation of the matrix, brittle failure of fibers and frictional sliding on the interface). It was assumed that the interface strength is negligible, and that the fiber/matrix interaction is controlled by friction. The simulation results were compared with experiments (load-CMOD curve), and a good agreement between experimental and numerical results was observed. Summarizing this short overview, one may state that the continuum mechanical finite elements models allow the incorporation of many different features of the nonlinear material behavior and the analysis of the interaction of available and evolving microstructural elements. More detailed overviews of the models of damage and fracture of fiber reinforced composites are given elsewhere [1, 21].

In the following work, we employ the continuum mechanics based, micromechanical, numerical methods to simulate the damage evolution in unidirectional, glass fiber reinforced polymer composites, and to analyze the effect of phase properties and the interaction between different damage modes in composites.

3. Automatic generation of 3D FE unit cell models of composites and modeling of damage evolution

3.1 Automatic generation of 3D FE models of FRCs: "Program "Meso3DFiber".

A special program code "Meso3DFiber" [1], which allows to automate the generation of 3D micromechanical finite element models of composites, was developed. The program, written in Compaq Visual Fortran, generates a command file for the commercial software MSC/PATRAN. The parameters of the model (volume content and amount of fibers, probabilistic/constant distributions of fiber radii, availability of interphase, etc.) are introduced interactively. The fibers in the unit cells were placed randomly in X and Y directions, using the random number

generator. The command file is played with PATRAN, and a 3D microstructural (unit cell) model of the composite with pre-defined parameters is generated. The finite element meshes are generated by sweeping the corresponding 2D meshes on the surface of the unit cell.
Figure 1 shows a micrograph of fracture surface of an unidirectional fiber reinforced composite with failed fibers (left) and an example of the generated FE models with 20 fibers, and removed layers of potential fracturing (right).

3.2 Damage modeling: fiber cracking and interface damage.

In order to model the fiber cracking, we used the idea of introducing potential fracture planes (in form of damageable cohesive elements) in random sections of fibers, suggested by González and LLorca [19]. The random arrangement of the potential failure planes in this case reflects the statistical variability of the fiber properties. Following this idea, we introduced damageable layers in several sections of fibers. These layers have the same mechanical properties as the fibers (except that they are damageable). The locations of the damageable layers in the fibers were determined using random number generator with the uniform distribution. The advantage of introducing thin, but 3D layers over cohesive surfaces (as in [19]) is that this approach allows the automatic random placement of the damageable layers at the stage of the mesh generation.

A similar concept was used to simulate the interface cracking of composites. Given that surfaces of fibers can be rather rough [25], and the interface regions in many composites contain interphases [26, 27], the interface debonding was considered not as a two-dimensional opening of two contacting plane surfaces, but rather as a three-dimensional process in a thin layer. Thus, the interface was represented as a “third (interphase) material layer” between the homogeneous fiber and matrix materials (compare [15]). The thickness of the interface layer was taken 0.2 mm, but can be varied in further simulations. Figure 2 shows examples of multifiber unit cells with 20 fibers and interphase layer (yellow).

3.3 Subroutine for damage simulation.

The damage evolution in the damageable layers, placed in random sections of fibers, as well as in the matrix and interphase layers was modeled using the finite element weakening method [20, 22-23]. The idea of this approach is that the stiffness of finite elements is reduced if a stress or a damage parameter in the element or a nodal point exceeds some critical level. This approach has been realised in the ABAQUS subroutine User Defined Field [20, 23].

In this subroutine, the phase to which a given finite element in the model is assigned, is defined through the field variable of the element. Depending on the field variable, different failure conditions are assigned by the subroutine to each finite element of the model. The subroutine checks whether the element failed or not, according to the properties of the matrix, interphase and fibers. Another field variable characterizes the state of the element (“intact” versus “damaged”). If the value of the damage parameter or the principal stress in the element exceeds the corresponding critical level, the second field variable of the element is changed, and the Young modulus of this element is set to a very low value (50 Pa, i.e., about 0.00001% of the initial value). The numbers of failed elements are printed out in a file, which can be used to visualize the calculated damage distribution. Both Weibull distribution of the strengths of each finite elements in fibers and of whole fibers, as well as constant fiber strength, uniform and Gaussian distributions are included into the subroutine, and can be tested in the simulations.

3.4 Properties of phases.

The following properties of the phases were used in the simulations. The glass fibers behaved as elastic isotropic solids, with Young modulus E_P=72 GPa, and Poisson’s ratio 0.26. The failure strength of glass fibers was assumed to be distributed by Weibull probability law [29], with parameters σ_0=1649 MPa and m=3.09 [29].

The elastic properties of the epoxy matrix were as follows: Young modulus 3790 MPa, Poisson's ratio 0.37, bulk modulus 5 GPa, instantaneous shear modulus 1.38 GPa [30, 31]. The viscoelastic properties were described by a single term Prony series, with the relaxation time 0.25 sec, and the modulus ratio g=0.125 [30, 31]. The failure stress of epoxy matrix was taken to be 67 MPa [33]. The properties of the interface/interphase layer were taken as averaged properties of the fibers and matrix, and were varied in some computational experiments.

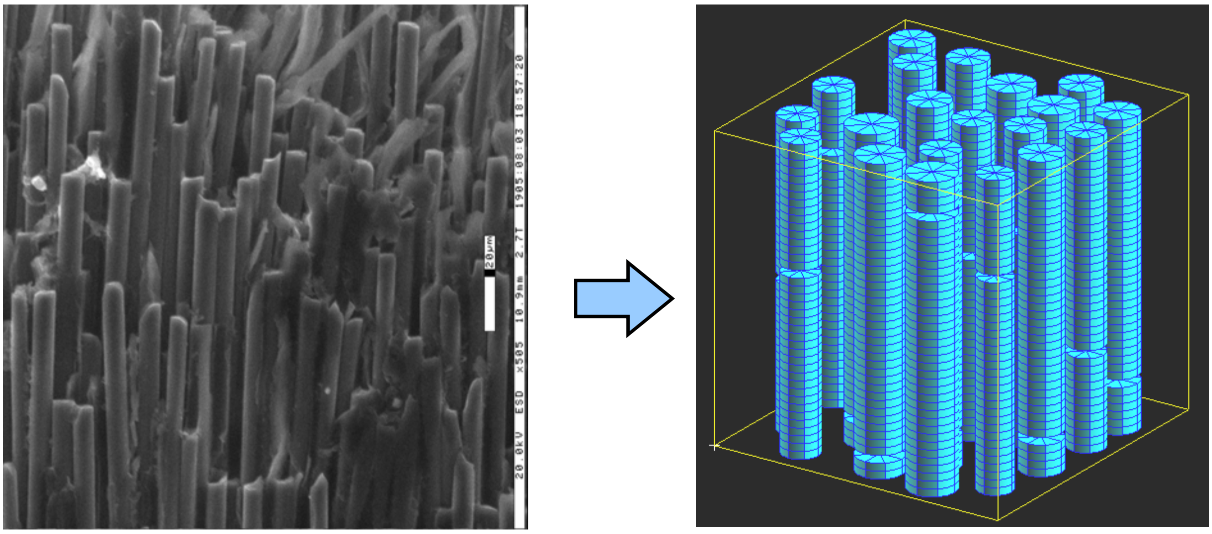

Figure *1. Micrograph of fracture surface of an unidirectional fiber reinforced composite (with failed fibers) (left) and an example of the generated FE models with 20 fibers, and removed layers of potential fracturing (right). Left picture presents carbon fibers in the polyester matrix (Courtesy of Dr. S. Goutianos, Risø National Laboratory, Denmark).*

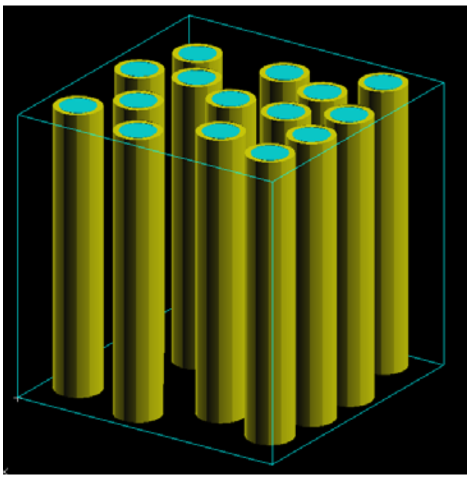

Figure *2. Examples: unit cells with 20 fibers and interphase (yellow) layers*

4. Computational experiments: Effect of phase properties on the strength and damage behavior of glass fiber reinforced polymer composites

In this section, we investigate the effect of the phase properties on the damage evolution and mechanisms in the cracks in the glass fiber reinforced polymer composites, using computational experiments.

A number of three-dimensional multifiber unit cells have been generated automatically with the use of the program “Meso3DFiber” and the commercial code MSC/PATRAN. The dimensions of the unit cells were 10 x 10 x 10 mm. The cells were subject to a uniaxial tensile displacement loading, 1 mm, along the axis of fibers (Z axis). As output results, the stress-strain curves and the damage strain curves were obtained, as well as the stress and strain, and damaged element distributions in the unit cells. The simulations were done with ABAQUS/Standard.

4.1 Damage evolution in composites with randomly distributed fiber strengths

The deformation and damage in the unit cells were simulated numerically. Unit cells with 20 fibers were subject to a vertical loading. Simulations with randomly (Weibull) distributed fiber strengths have been carried out. The parameters of the Weibull distribution are given above. At this stage of the work, the very strong fiber/matrix interface bonding was assumed, and only the effect of the matrix cracks on the fiber fracture was studied.

In the simulations, both fiber failure and matrix cracking have been observed. Figure 3 shows the von Mises stress field in the fibers before the first fiber failure (a), and after the failure of two fibers (ε=0.012) (b). After the third fiber cracking, a matrix crack forms in the vicinity of a fiber crack. Figure 4 shows the formation of the matrix crack from the fiber crack (a), and the matrix crack growth from the fiber crack to the neighboring fibers (b, c).

Figure 5 shows the load sharing and localization around a failed fiber, after the first fiber failure. The higher stresses on the fibers adjacent to the failed fiber can be seen.

Figure 6 shows the damage-strain curve for this model. One can see that damage growth in the matrix begins somewhat later than the cracking in fibers, and is in fact triggered by the fiber failure. However, the crack growth in matrix goes on much more quickly than that in fibers.

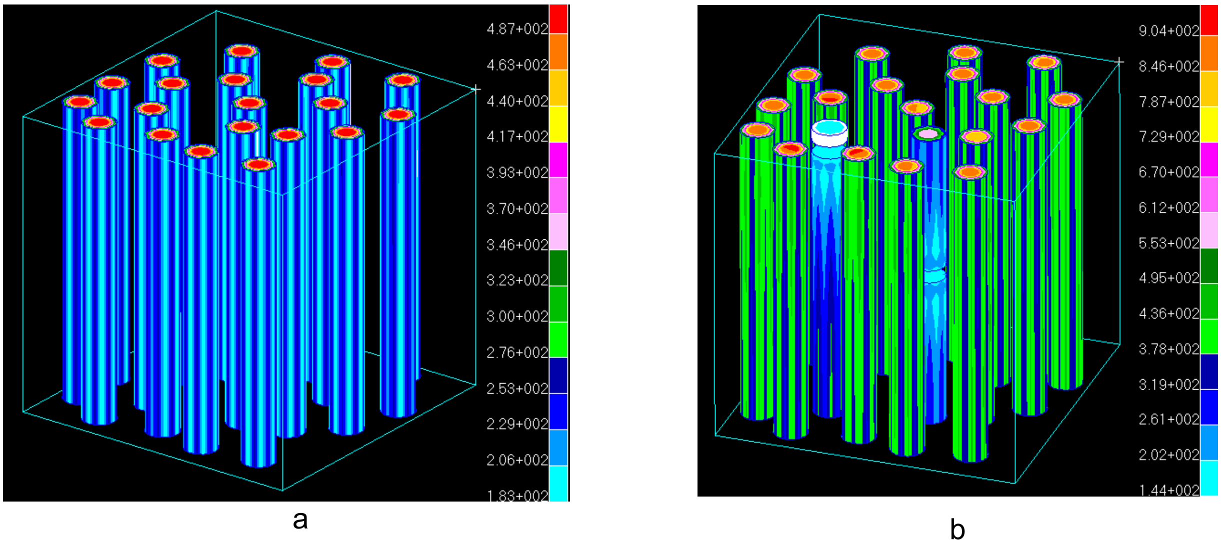

Figure 3. *Von Mises stress field in the fibers before the first fiber failure (a), and after after the failure of two fibers (ε=0.012) the first fiber failure (ε=0.008) (b), and three fibers (ε=0.013) (c, d).*

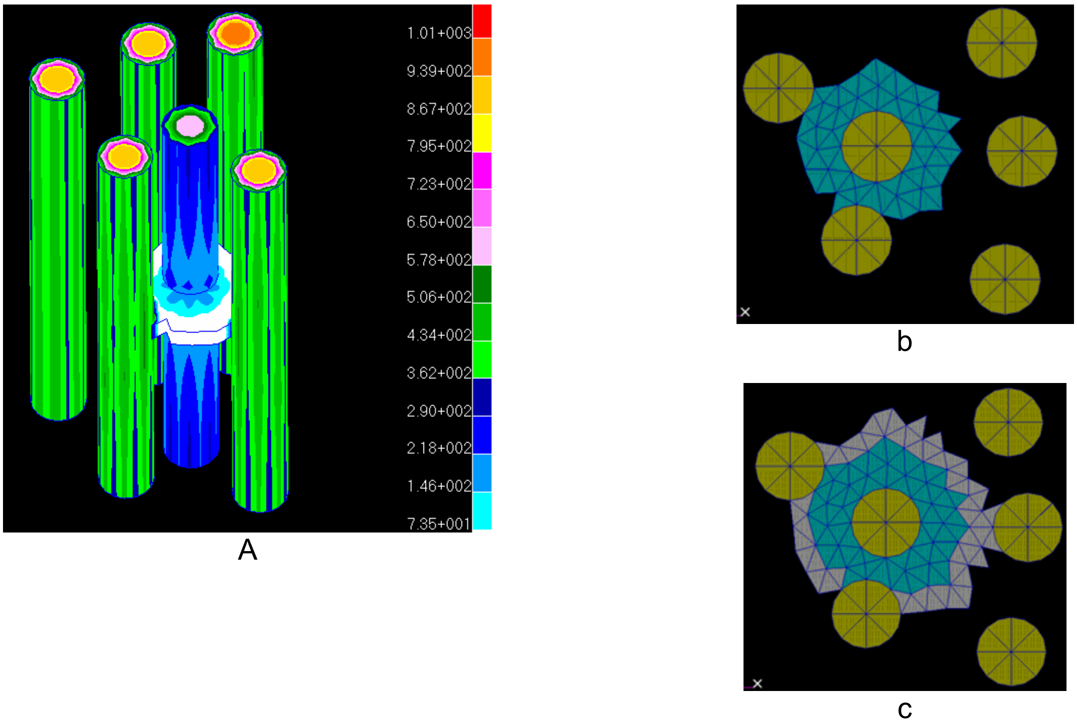

Figure 4. *Formation of the matrix crack from the fiber crack (a), and the matrix crack growth from the fiber crack to the neighboring fibers (b, c).*

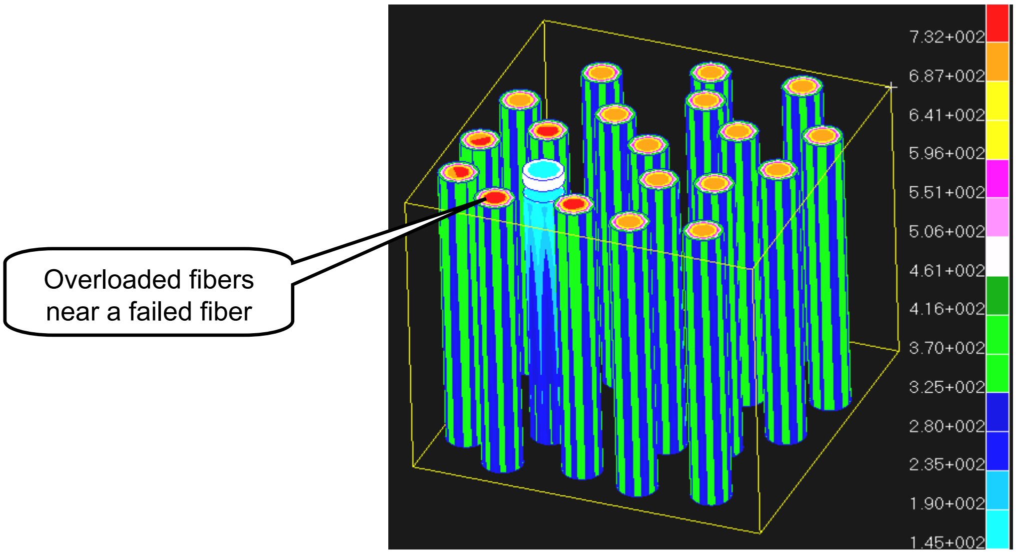

Figure *5. Load sharing and localization around a failed fiber (after the first fiber failure, ε=0.008)*

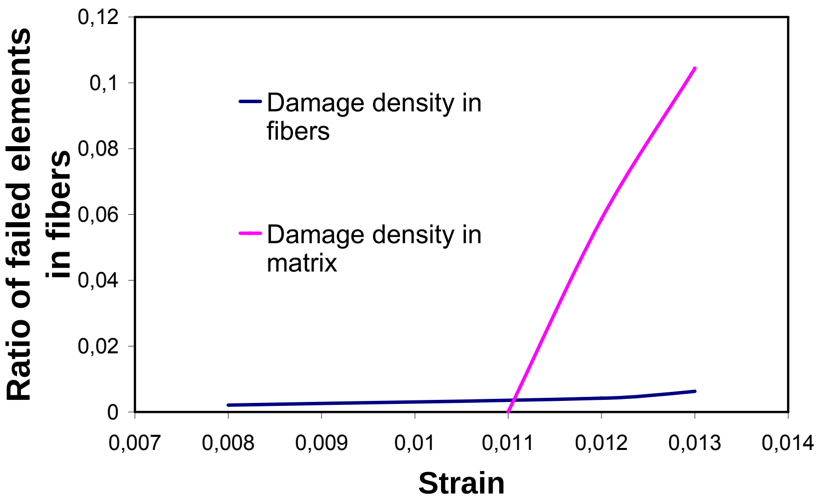

Figure 6. D*amage-strain curves: the matrix cracking is triggered by the fiber failure, but the crack in matrix grows much quicker than the cracks in fibers*

4.2 Effect of the statistical variability of fiber strengths on the damage evolution in composites

In this section, the comparison of the mechanical and damage behavior of composites with randomly (Weibull) distributed fiber strengths, and the constant fiber strength is carried out. The parameters of the Weibull distribution of fiber strengths was taken σ_0=1649 MPa, and m=3.09, as above. For the case of the constant fiber strength, the strength value was calculated as a mean value of the Weibull distribution, by formula: $\sigma_{av} = \sigma_0 \Gamma(1+1/m) = 1474$ MPa.

Figure 7 shows the von Mises stress distribution in the fibers after their cracking for the case of constant fiber strength. The stress-strain and damage strain curves are shown in Figure 8. On the basis of the simulations, one can conclude that homogeneous fibers ensure higher strength of a composite at the pre-critical load. However, the fibers with randomly distributed strengths lead to the higher strength at post-critical loads.

These simulations lead us to the idea that a combination of fibers with constant (or only slightly varied) strengths and those with highly variable strengths can be used to ensure high damage resistance of composite both at pre- and post-critical loads.

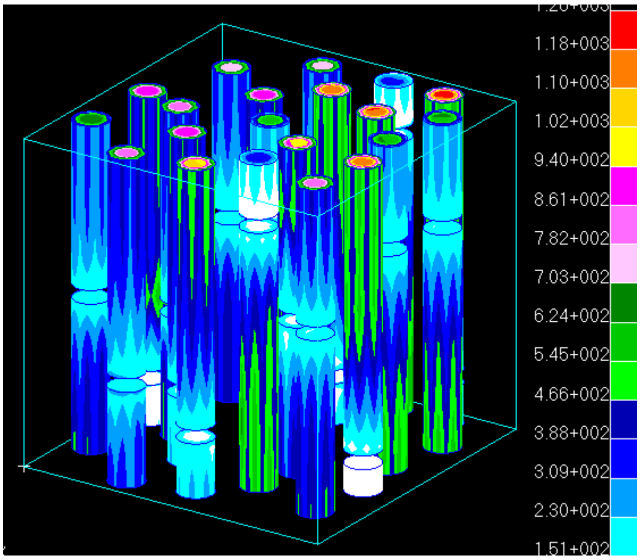

Figure 7. *Von Mises stress distribution in fibers after cracking for the case of constant fiber strength*

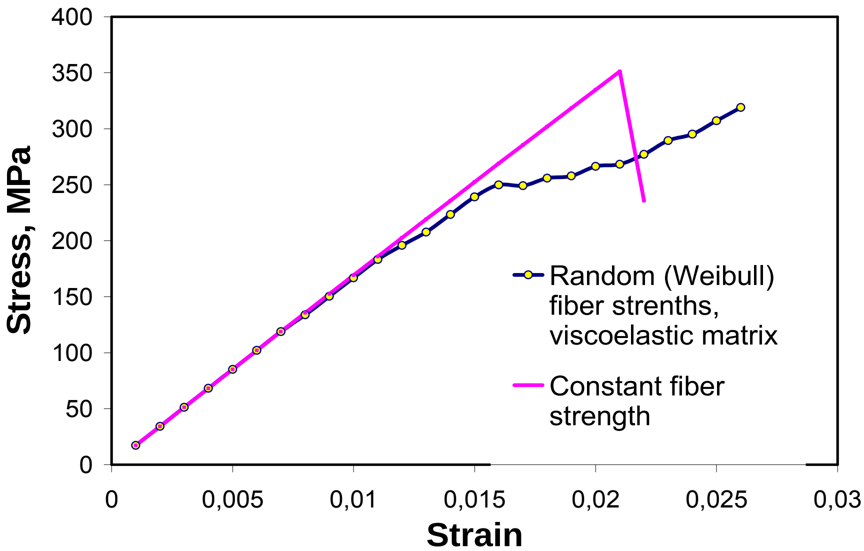

A

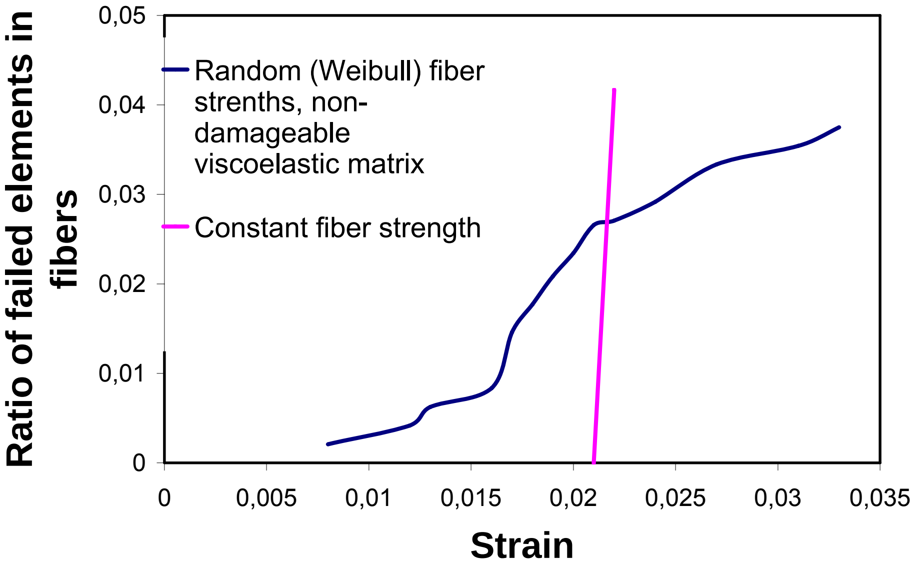

b

Figure 8. *Stress-strain and damage strain curves: random (Weibull) and constant fiber strengths.*

4.3 Effect of the viscosity of the matrix on the damage evolution

Here, we seek to investigate the effect of the matrix viscosity on the damage evolution in fibers. The unit cell model with a viscoelastic matrix, as described above, was compared with a model with an elastic matrix, having the same elastic properties (E= 3790 MPa, and v=0.37).

The stress-strain and damage strain curves for the case of are shown in Figure 9. One can see that the viscosity of matrix leads to higher strains (at the same stress level) and higher damage rate in fibers, as compared with elastic matrix. This difference is observed only after the beginning of the damage evolution in fibers, and becomes more pronounced the more fibers get damaged. For instance, the damage density in fibers in the composite with viscoelastic matrix is 5% higher at applied stress 300 MPa than that in the composite with a purely elastic matrix.

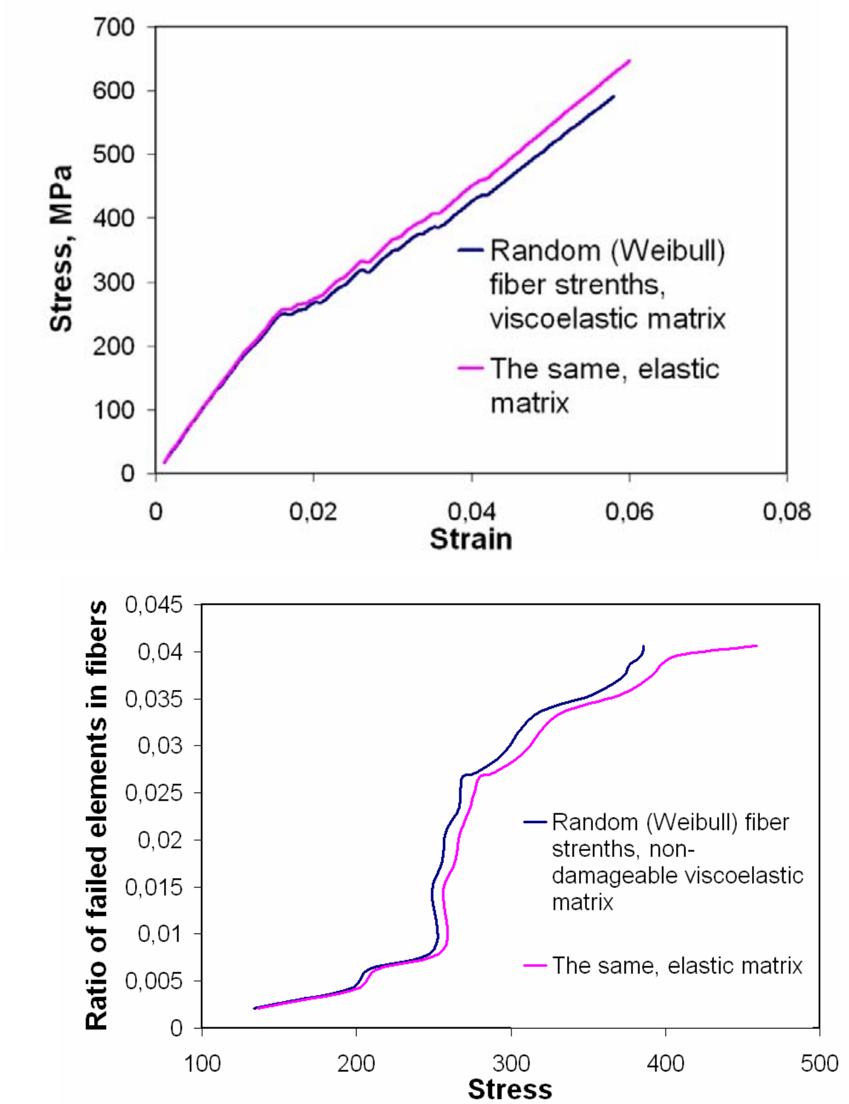

Figure 9. *Stress-strain and damage strain curves: viscous matrix and the elastic matrix (with the same elastic coefficients)*

5. Influence of defects in the composites on the strength and damage resistance: Numerical analysis

5.1 Effect of matrix defects on fiber cracking

In this section, we investigate the effect of matrix cracks on the fiber fractures. Three versions of the unit cells (with 20 fibers) were generated, containing large matrix cracks, bridged by intact fibers. The matrix cracks were oriented horizontally, normal to the fiber axis and loading vector. The lengths of the cracks were taken 1.6 mm (1/6 of the cell size), 4.1 (5/12 of the cell size), 6.6 mm (8/12 of the cell size). The crack opening was taken 1/12 of the cell size (0.8 mm). Figure 10 shows the general appearance of the cells with matrix cracks.

Figure 11 shows the von Mises stress distribution in the matrix and fibers, and the maximal shear strain in the matrix with the long crack after the fiber failure. The stresses are very high in the bridging fibers, and in the matrix regions between two neighboring fiber cracks. In Figure 11b, the regions of high strain level (shear bands) are seen, which connect the crack tip in the matrix with the cracks in fibers, and the fiber cracks in neighboring fibers.

Figure 12 gives the stress-strain curves and the damage (fraction of damaged elements in the damageable sections of the fibers) versus strain curves. The stiffness reduction due to the fiber cracking is more pronounced in the cells with long cracks that in the cells with short or no matrix crack (13% higher stiffness in the case of intact matrix, than in the case of the matrix with a long crack).

It is of interest that the damage growth in fibers seems to be independent from the crack length in matrix. In order to validate this result, we use the observations of Venkateswara Rao et al. [36]. Venkateswara Rao and colleagues demonstrated experimentally that fiber reinforced composites are insensitive to the presence of notches under tension loading. This experimental result conforms our theoretical simulations.

However, the weak influence of the matrix cracks on the fiber fracture in this case is in strong contrast to our other results obtained for the case of the constant fiber strength and ductile (aluminium) matrix, presented in [35]. In this work, a strong effect of the matrix crack length on the damage growth and the stress-strain curve of the composites was observed. In order to separate out the effect of the ductile matrix and the constant fiber strength, we carried out the simulations (similar to above) with the constant fiber strength. Figures 13 and 14 give the stress-strain curves and the damage versus strain curves for the case of constant fiber strengths. The curves for randomly distributed fiber strengths are given for comparison as well. It can be seen that the matrix cracks do influence the beginning of fiber cracking and the peak stress, if the fiber strength is constant. In the composites with constant fiber strengths, fiber fracture begins much earlier if the matrix is cracked than in the case of intact matrix. Generally, fiber cracking begins the earlier the longer crack in the matrix. The critical strain, at which the stiffness of composite is stepwise lowered, is independent on the length of the matrix cracks.

One may state that the matrix cracks have an effect somewhat similar to the statistical variability of fiber strengths: they make the material weakening during the failure process smooth and nonlinear.

The main conclusion from the above simulations is that the statistical variability of fiber strengths has stronger effect on the damage evolution in the composites, than the matrix cracks and their sizes. Thus, the variability of the fiber properties supersedes the effect of matrix cracks on the composite strength.

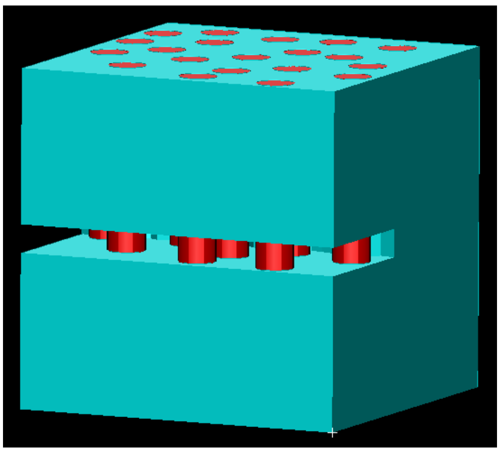

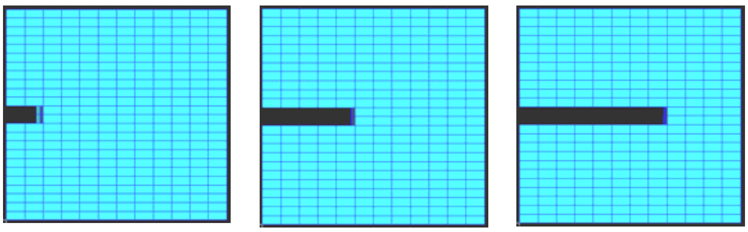

Figure *10. Unit cell with a matrix crack and bridging fibers [1, 35]*

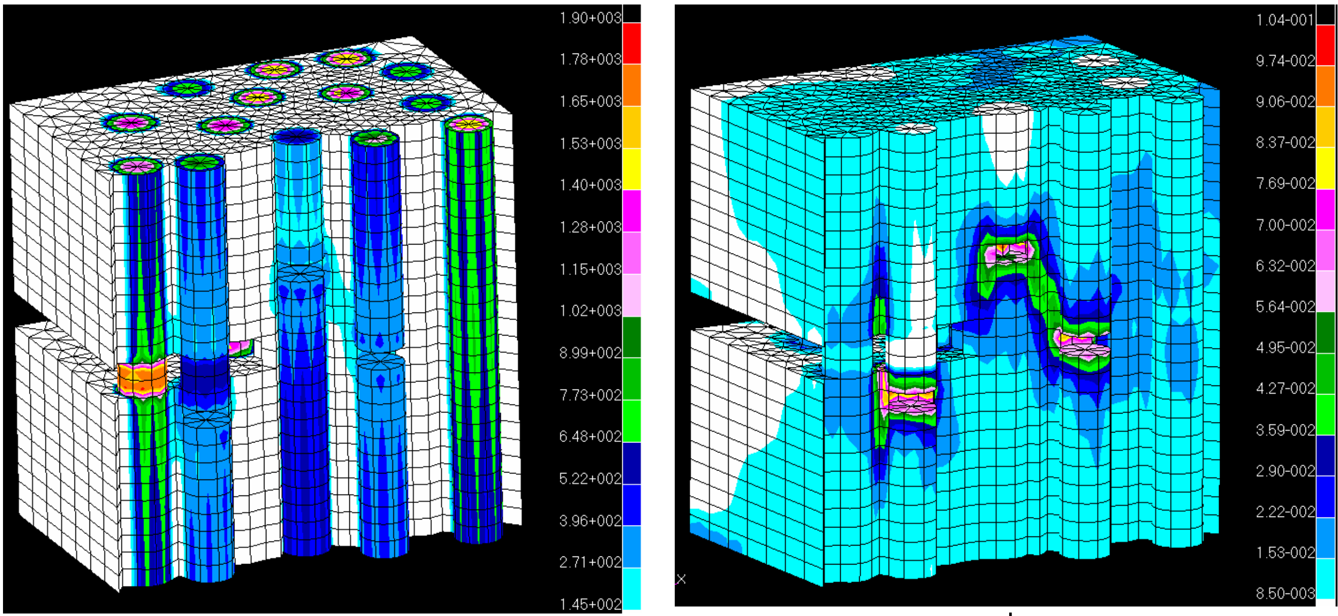

b

Figure *11. Von Mises stress distribution in the fibers and matrix (a), and maximal shear strain in the matrix (b) after the fiber cracking*

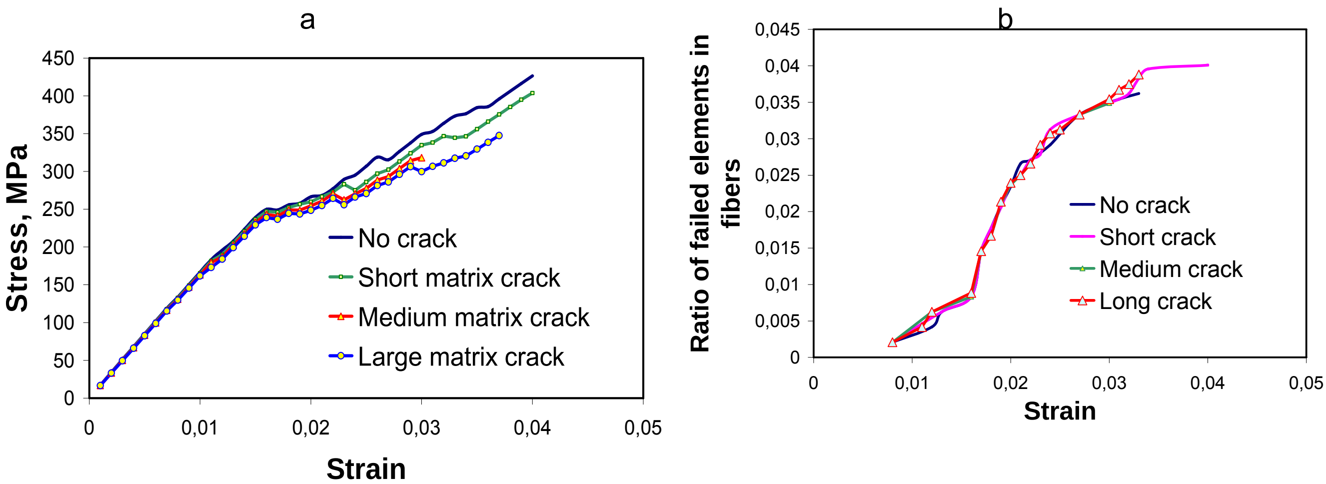

Figure *12. Stress-strain (a) and damage (fraction of damaged elements in the damageable sections of the fibers) versus strain (b) curves for the unit cells with and without the matrix cracks.*

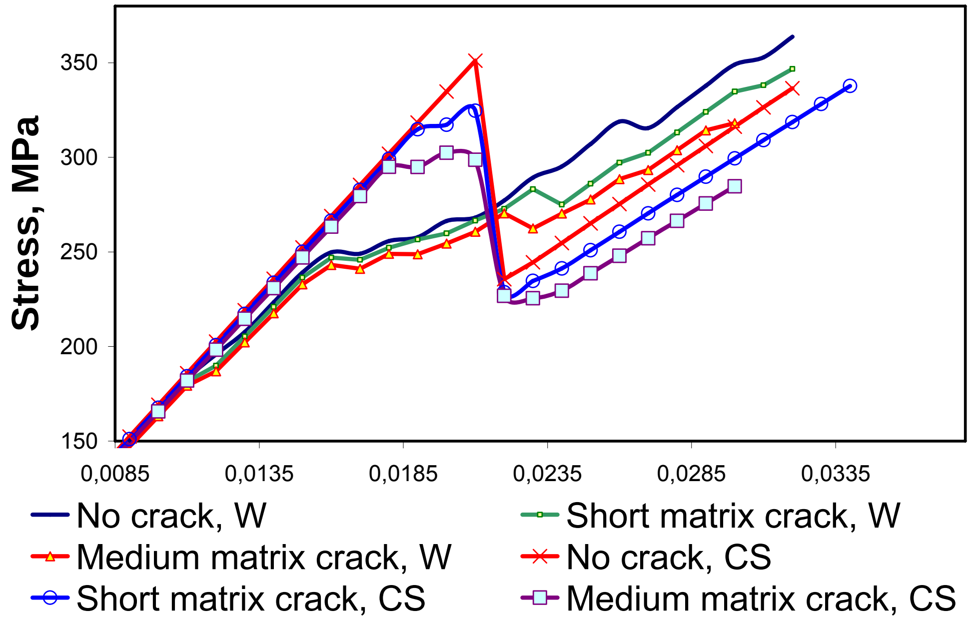

Figure *13. Stress-strain curves for the unit cells with and without the matrix cracks, with constant (CS) and randomly distributed (W-Weibull) strengths of fibers.*

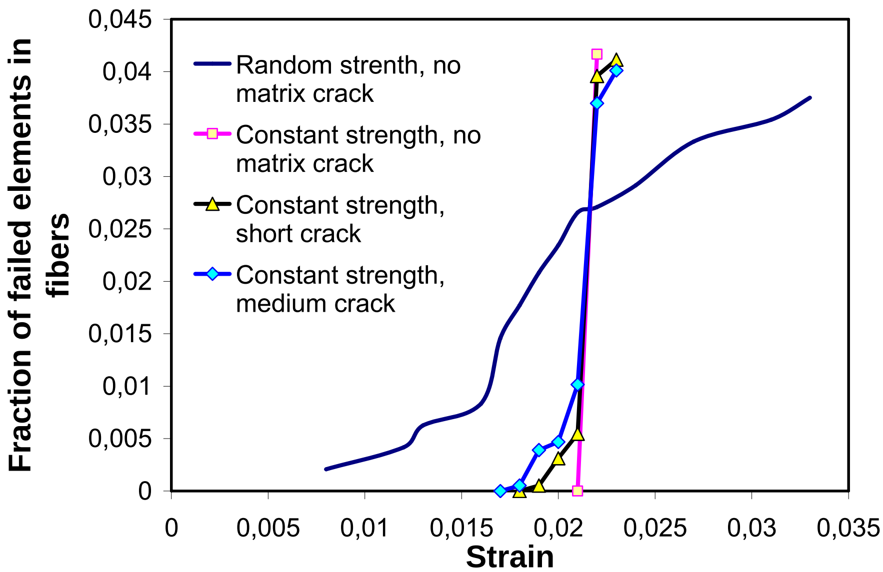

Figure *14. Damage (fraction of damaged elements in the damageable sections of the fibers) versus strain curves for the unit cells with and without the matrix cracks, with the constant strength of fibers. A curve for randomly distributed fiber strengths is given for comparison.*

5.2 Matrix defects and their influence on interface damage

Let us consider the interaction between the damage growth in the interface layer and the matrix defects. A number of unit cells (with 15 fibers and 25% fiber volume content) were generated, and subject to the axial loading. The intact, but damageable interface layers are considered. The thickness of the interface layer was taken 0.2 mm. The interface layer was assumed to be a homogeneous isotropic material, with Young modulus 37.9 GPa (i.e., the average value of the Young moduli of fiber and matrix materials) and Poisson’s ratio of the matrix. As a first approximation, we chose the maximum principal stress criterion for the interface damage (therefore, assuming rather brittle interface). As noted in [35], the homogeneous representation of the interphase layer can be considered only as a first approximation, and the model can be further improved if the graded material model is used to represent the interface layer, with properties to be determined from the inverse analysis [1].

First, we considered the case of intact, strong and tough matrix, and damageable fibers and interface layers. Figure 15 shows the damage evolution in the fibers and matrix, observed in the simulations for the case of critical stress of interface layer 550 Mpa. One can see that the formation of the interface cracks takes place after the fiber cracking, and in the vicinity of the fiber cracks. Thus, the formation of interface cracks is triggered by the fiber cracks. After an interface crack is formed, it can cause the formation of other interface cracks near neighbouring fibers (in the case of relative weak interfaces).

Further, the simulations of the damage evolution in the unit cells with differently strong interface layers and with and without bridged matrix cracks have been carried out. Several levels of the critical stress of interface layer have been taken: 100, 150, 250, 400, 550 and 750 MPa (the last value corresponds to the mean value of the average strengths of fibers and the matrix). The unit cells with the matrix cracks (notches) had the crack length of 0.3 (short crack) and 0.58 of the cell size (long crack). The fiber arrangement in the cells with and without matrix cracks was the same. The stress-strain curves, damage-strain curves for the fibers and interfaces have been obtained.

Figure 16 shows some representative interface damage-applied strain curves for the cases of the interfaces with different strengths (100, 250, 400, 770 MPa). Both the cases with and without the matrix crack are considered. For the interface strengths of 400, 500 (not shown) and 770 MPa (“strong interfaces”), the stress-strain curves as well as the damage-strain curves of fibers are almost identical in the cases with and without matrix cracks. Apparently, the degradation of composite in this case is fully controlled by the fiber strength and failure. When the fibers fail, it leads to the interface damage (compare Figure 15).

However, in the case of a weak interface (100, 150 and 250 MPa), the damage mechanism in the composite is changed. No fiber cracking is observed, but the interface damage begins much earlier, than in the case of the stronger interface. The interface damage in this case is clearly influenced by the matrix cracking. Thus, the interface properties influence the sensitivity of the composites to the matrix defects: in the case of the weak fiber/matrix interface, the matrix defects can speed up the cracking in fibers and the composite failure.

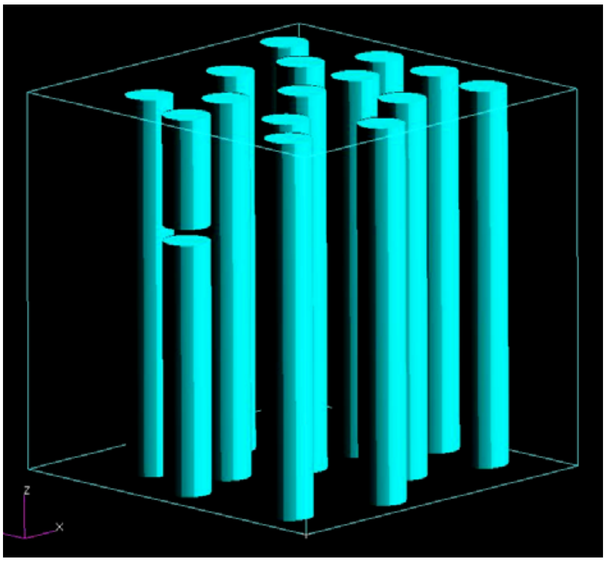

a

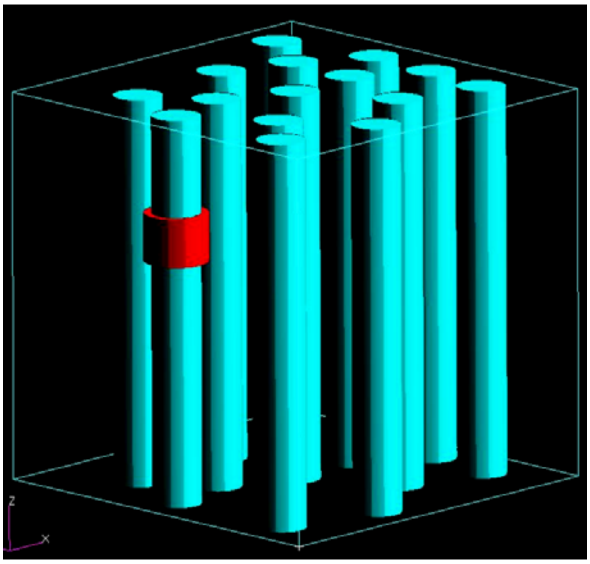

b

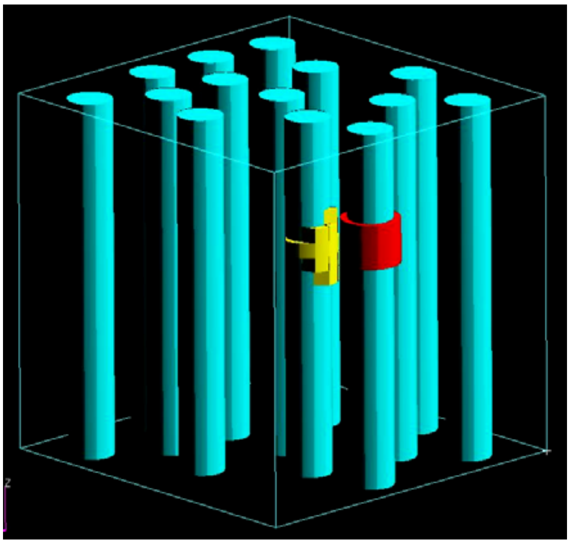

c

Figure ***15.*** *Damage evolutio in a composite with damageable interface and fibers, and strong matrix: (a) Fiber cracking, u=7e-3 mm, (b) Interface damage nearby the fiber crack, u=7.2e-3 mm, (c) Interface damage near the neighbouring fiber, u=9.4..9.8e-3 mm.*

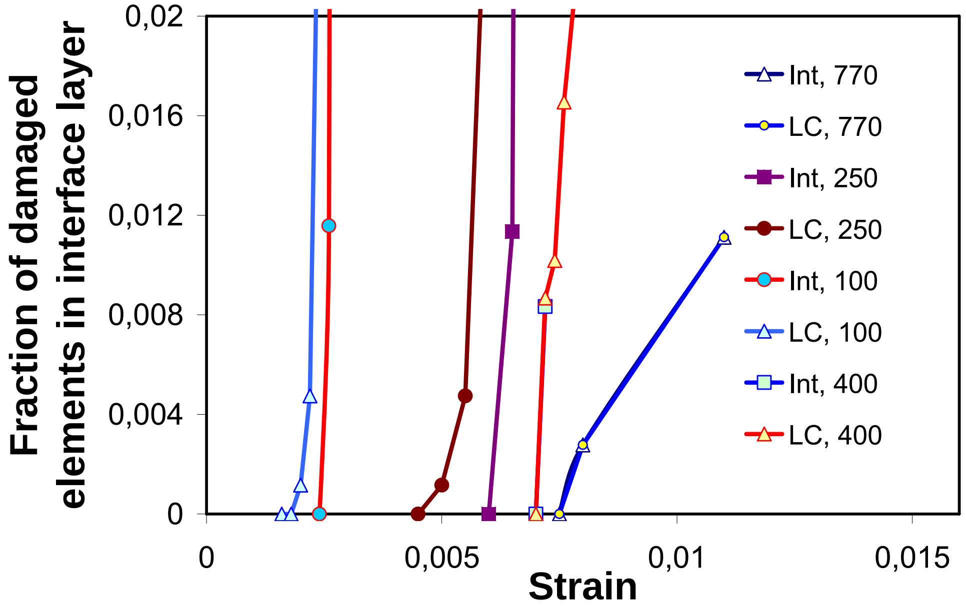

Figure *16. Representative damage-strain curves for interface damage for the interfaces with differently strengths (100, 250, 400 and 770 Mpa). The unit cells with no matrix crack (INT=intact matrix) and with a long matrix crack (0.58 of the cell size, LC=long crack) are considered.*

5.3 Interface defects and their influence on fiber cracking

In the previous section, we observed that the interface damage is triggered by the fiber cracking. In this section, we analyze the *effect of the pre-damaged interface* on the fiber cracking in the composite. A half-circular interface microcrack was introduced into an interface layer in the unit cell model with 15 fibers (Figure 17). The unit cell with the microdamaged interface was subject to a tensile loading. The critical stress in the interface was assumed to be 770 MPa.

Some results of the simulation are shown in Figure 18: the Mises stress distribution in a horizontal section of the cell (a) (u=0.0045 mm), in a vertical section of the fibers with intact and damaged interface layers before (b) and after (a) first fiber cracking (u=0.0075 mm), and the formation of interface cracks in the unit cell (d) (u=0.008 mm).

It is of interest that the damaged interface leads to a slightly lower stress level in the corresponding fiber: while the stresses in the vicinity of the interface crack are rather high, the far field stresses in the fiber are lower than those in fibers with undamaged interfaces. As a result, not the fiber with damaged interface fails first, but another fiber. It can be seen from Figure 18cd that the fiber crack (which took place not in the fiber with damaged interface, but in another fiber) leads to the interface damage just around the fiber crack.

Thus, we observe again that a microcrack in the interface layer does not cause the fiber cracking in the adjacent fiber, but even slightly reduces the load on the fiber (thus, reducing the likelihood of the failure of this fiber). In order to validate this conclusion, we use the observations by Feih et al. [37]. In their experimental investigations, Feih and colleagues observed “a shift to a later fragmentation onset with weaker interface bonding”, which was attributed to the “partial fiber debonding prior to first fiber fracture [which were observed during the fragmentation test], thereby resulting in a lower fiber strain and later fragmentation onset”. This confirms our results obtained in this section.

The fiber cracks cause interface damage, but not vice versa. (It should be stressed that this observation was made in the given case/ for given material properties, and the results in other cases can be different).

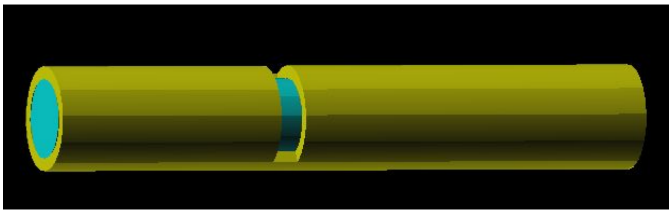

Figure 17. A half-circular microcrack in the interface layer

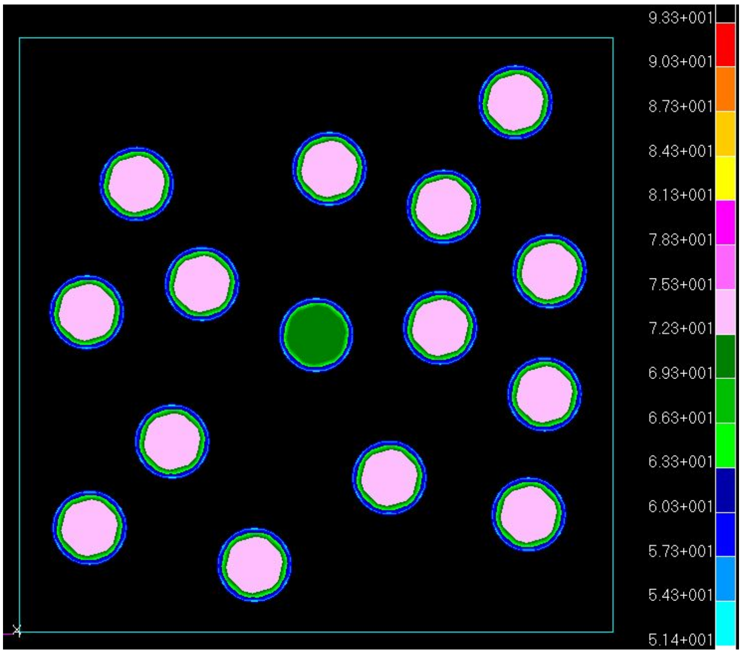

A

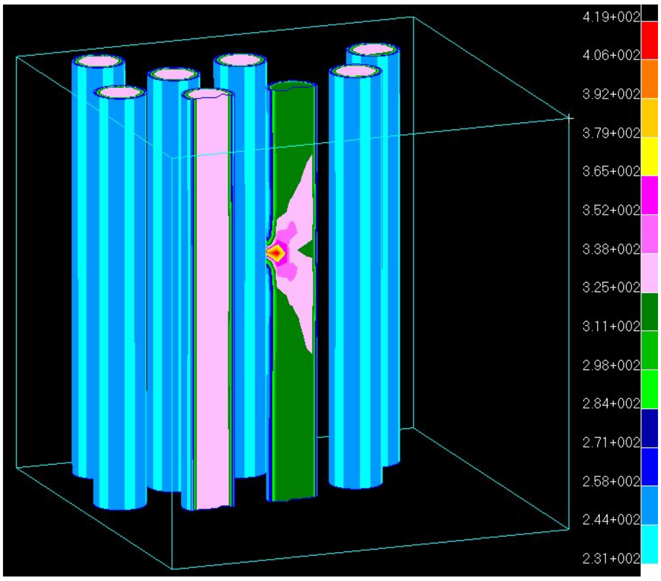
4.19+002
4.06+002
3.92+002
3.79+002
3.65+002
3.52+002
3.38+002
3.25+002
3.11+002
2.98+002
2.84+002
2.71+002
2.58+002
2.44+002
2.31+002

B

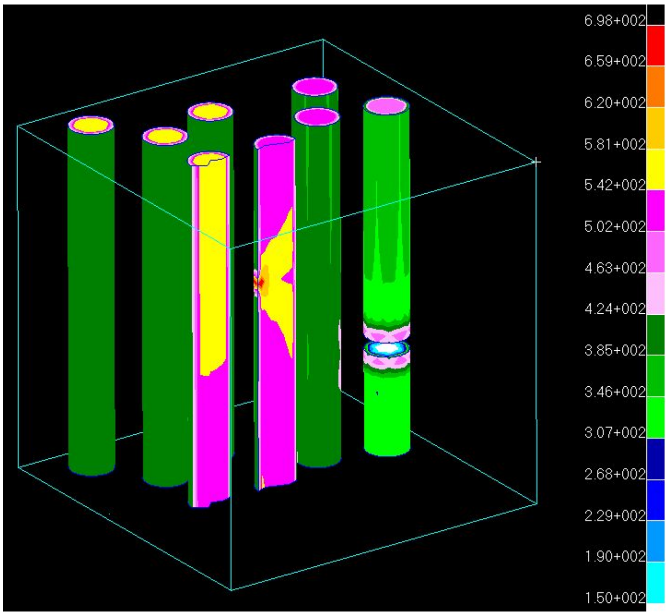
6.98+002
6.59+002
6.20+002
5.81+002
5.42+002
5.02+002
4.63+002
4.24+002
3.85+002
3.46+002
3.07+002
2.68+002
2.29+002
1.90+002
1.50+002

C

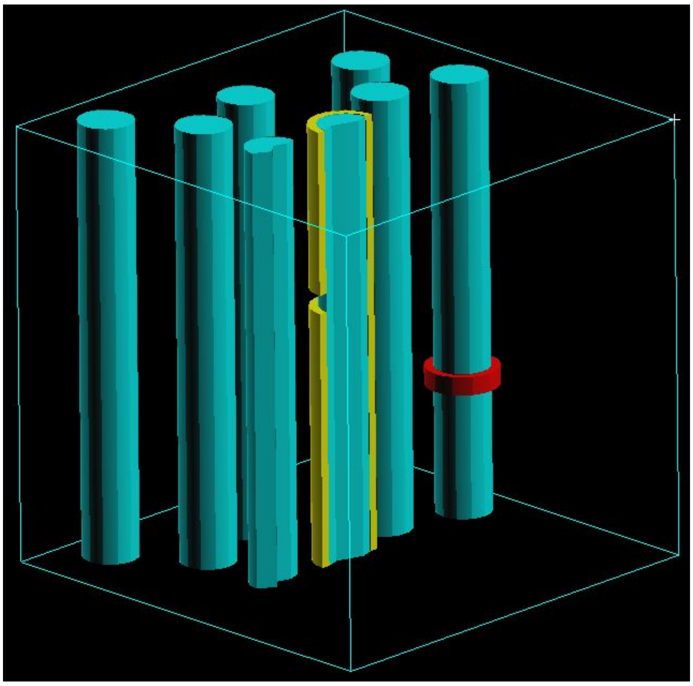

D

Figure *18. Stress distribution in the unit cell with microdamaged interface: the Mises stress distribution in a horizontal section of the cell (a), in a vertical section of the fibers with intact and damaged interface layers before (b) and after (a) first fiber cracking, and the formation of interface cracks in the unit cell (d).*

5.4 Competition between damage modes in composites

In this section, the interaction between all three damage modes in composites (matrix cracks, interface damage and fiber fracture) is considered.

Figure 19 shows the results of simulations: damage formation in the fibers, interface and matrix. The damage evolution begins by formation of a crack in a fiber and (in another, rather far site) in the matrix (u=0.1 mm). Then, the interface crack forms nearby the fiber crack, and the large matrix crack is formed (u=0.15 mm). Figure 20 shows the damage-strain curves for this case.

It is of interest that in the case when all the three damage mechanisms are possible, the competition between the matrix cracking and the interface debonding is observed. In the area, where the interface is damaged, no matrix crack forms; vice versa, in the area, where the long matrix cracks is formed, the fiber cracking does not lead to the interface damage.

Apparently, weak interfaces of a composite, as such, have a negative effect of the composite properties: ultimately, the homogeneously weak interfaces will debond and the composite will behave as a dry fiber bundle. However, the results of this and previous sections demonstrate that local weak places in composite interfaces can be rather beneficial for the composite strength and toughness: they can prevent the matrix failure (by channeling the fracture energy into interface defects), and even delay the fiber failure. Practically, it means that a heterogeneous interface (interface with both weak and strong regions) can prevent the matrix failure, and therefore, ensure the integrity of the material.

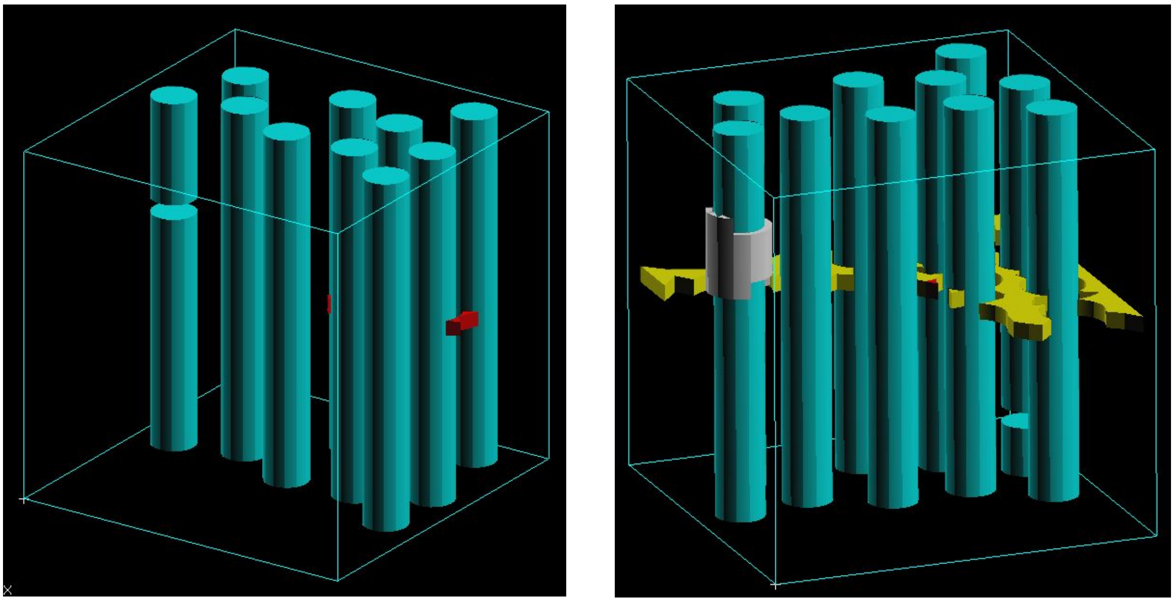

Figure *19. Competition of damage modes: (a) one failed fiber and a few microcracks in the matrix (red), u=0.1 mm, and (b) two fibers have failed, the interface crack is formed in the vicinity of a fiber crack and the matrix crack is formed (u=0.15 mm).*

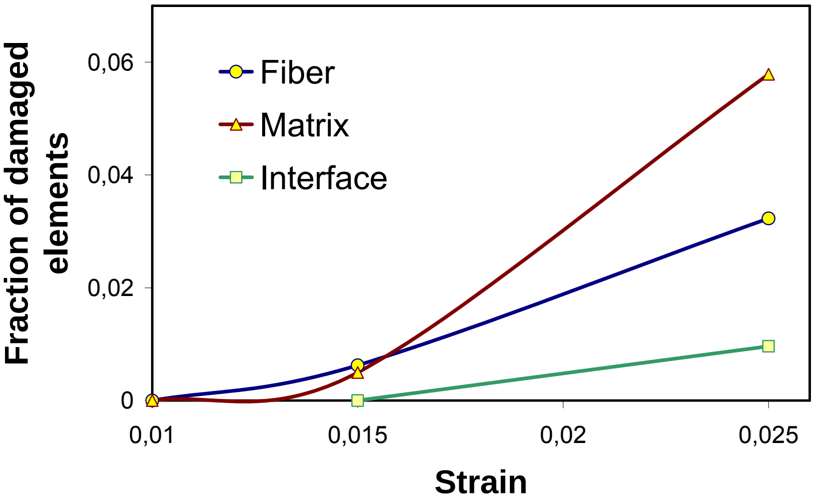

Figure *20. Damage-strain curves for the case of three acting damage mechanisms*

6. Conclusions

Numerical investigations of the damage evolution in glass fiber reinforced polymer matrix composites are used to analyse the interplay of damage mechanisms (fiber, matrix, interface cracking) and the effect of local properties on the microscopic damage mechanisms. The computational investigations lead us to following conclusions:

- Fibers with constant strength ensure higher strength of a composite at the pre-critical load, while the fibers with randomly distributed strengths lead to the higher strength of the composite at post-critical loads.
- The viscosity of the matrix leads to the higher damage rate in fibers, as compared with the elastic matrix.
- The influence of the matrix defects on the composite strength is much weaker than the effect of the statistical variability of fiber strengths. If the fiber strength is constant, the fiber cracking begins the earlier, the longer is the matrix crack. In the case of randomly distributed fiber strengths, the damage growth in fibers seems to be almost independent from the crack length in matrix, and fully controlled by the load redistribution from weak and failed to remaining fibers.
- Interface cracks have a remarkable effect on other damage modes (as fiber and matrix cracking): no matrix crack formed near the fibers with damaged interfaces; vice versa, in the area, where the long matrix cracks is formed, the fiber cracking does not lead to the interface damage. Further, it was observed that the damaged interface causes slightly lower stress level in adjacent fibers, what can lead to the situation when other fibers, with intact interfaces fail first. Practically, these observations suggest that an interface with varied strengths and weak local areas can delay the matrix failure and even fiber failure, and therefore, ensure the higher strength of the composite.

References:

1. Mishnaevsky Jr. L. (2007) Computational Mesomechanics of Composites, John Wiley and Sons, London, 280 pp.
2. Cox H.L. (1952) The elasticity and strength of paper and other fibrous materials. Brit. J. Appl. Phys. 3, pp. 73-79
3. Sastry, A. M., and S. L. Phoenix (1993) Load redistribution near non-aligned fiber breaks in a 2-D unidirectional composite using break-influence superposition. Materials Science Letters 12, pp.1596-99
4. Xia Z., Curtin W. A. and Okabe T.(2002) Green's function vs. shear-lag models of damage and failure in fiber composites , Composites Science and Technology, Vol. 62, 10-11, pp. 1279-1288
5. Daniels, H. E. (1945) The statistical theory of the strength of bundles of threads, Proc.Royal Society London A 183, 405
6. Kun, F., Zapperi, S., and Herrmann, H. J. (2000) Damage in fiber bundle models. European Physical Journal B17, pp. 269-279, Raischel, F., Kun, F. and Herrmann, H.J. (2006) Failure process of a bundle of plastic fibers, Physical Review E 73, 066101 -12
7. Marshall D. B., Cox B. N. and Evans A. G. (1985) The mechanics of matrix cracking in brittle-matrix fiber composites, Acta Metall. 33, 2013-2021
8. Budiansky, J.W. Hutchinson and A.G. Evans, Matrix fracture in fiber-reinforced ceramics, Journal of Mechanics and Physics of Solids 34 (1986) (2), pp. 167–189.
9. McCartney L. N., (1987) Mechanics of matrix cracking in brittle-matrix fiber-reinforced composites, Proc. R. Soc. London, A, 409,329-50 (1987)
10. Allen, D.H., C.E. Harris and S.E. Groves. 1987. A thermomechanical constitutive theory for elastic composites with distributed damage-I, Int. J. Solids Structures, 23:1301-1318
11. Burr, A., Hild, F., Leckie, F. Continuum description of damage in ceramic-matrix composites. European J. Mechanics A/Solids. Vol 16. Pages 53-78. 1997
12. Brockenborough, J.R., Suresh, S. and Wienecke, H.A., (1991) Deformation of metal-matrix composites with continuous fibers: Geometrical effects of fiber distribution and shape, Acta Metallurgica et Materialia, 39 (5), pp. 735-752

13. Böhm, H.J. and Rammerstorfer, F.G. (1993) Micromechanical models for investigating fibre arrangements in MMC's, Proc Int. Seminar "Micromechanics of Materials" (MECAMAT), pp. 383-394
14. I. Babuška, B. Andersson, P. J. Smith and K.Levin (1999) Damage analysis of fiber composites Part I: Statistical analysis on fiber scale, Computer Methods in Applied Mechanics and Engineering, Vol. 172, 1-4, pp. 27-77
15. Asp L. E., Berglund L. A. and Talreja R. (1996) Effects of fiber and interphase on matrix-initiated transverse failure in polymer composites, Composites Science and Technology Vol. 56, 6 , pp. 657-665
16. Vejen N. and Pyrz R. (2002) Transverse crack growth in glass/epoxy composites with exactly positioned long fibres. Part II: numerical, Composites Part B: Engineering, Vol. 33, 4, pp. 279-290
17. J. A. Sherwood and H. M. Quimby (1995) Micromechanical modeling of damage growth in titanium based metal-matrix composites, Computers & Structures, Vol. 56, 2-3, pp. 505-514
18. Zhang X., Liu H.Y.and Mai Y.W. (2004), Effects of fibre debonding and sliding on the fracture behaviour of fibre-reinforced composites, Composites Part A: Applied Science and Manufacturing, Vol. 35, 11, pp.1313-1323
19. Gonzalez, C. and LLorca, J. (2006) Multiscale modeling of fracture in fiber-reinforced composites Acta Materialia, 54, pp. 4171–4181
20. L. Mishnaevsky Jr and S. Schmauder, Continuum Mesomechanical Finite Element Modeling in Materials Development, Applied Mechanics Reviews, Vol. 54, 1, 2001, pp. 49-69
21. L. Mishnaevsky Jr and P. Brøndsted, Micromechanical Modeling of Strength and Damage of Fiber Reinforced Composites, Annual Report on EU FP6 Project UpWind Integrated Wind Turbine Design (WP 3.2), Risø National Laboratory, DTU, 2007
22. L. Mishnaevsky Jr, Automatic voxel based generation of 3D microstructural FE models and its application to the damage analysis of composites, Materials Science & Engineering A, Vol. 407, No. 1-2, 2005, pp.11-23
23. L. Mishnaevsky Jr, Functionally gradient metal matrix composites: numerical analysis of the microstructure-strength relationships, Composites Sci. & Technology, 2006, Vol 66/11-12 pp 1873-1887
24. L. Mishnaevsky Jr, Damage and fracture of heterogeneous materials, Balkema, Rotterdam, 1998, 230 pp.
25. O. K. Buryan and V. U. Novikov, Modeling of the Interphase of Polymer-Matrix Composites: Determination of Its Structure and Mechanical Properties, Mechanics of Composite Materials, Vol. 38, No. 3, 2002, 187-190
26. Downing T. D. , Kumar R. , Cross W. M. , Kjerengtroen L. and Kellar J. J. (2000) Determining the interphase thickness and properties in polymer matrix composites using phase imaging atomic force microscopy and nanoindentation, J. Adhesion Science and Technology, Vol. 14, 14, pp. 1801-1812
27. Huang Y, Petermann J (1996) Interface layers of fiber-reinforced composites with transcrystalline morphology. Polymer Bulletin, 36(4), pp.517-524
28. Agarwal B. D. and Broutman L. J., 1990, Analysis and performance of fiber composites, Second Ed., Wiley, New York, 449 pp.
29. S. Feih, A. Thraner, H. Lilholt, Tensile strength and fracture surface characterisation of sized and unsized glass fibers, J of Materials Science 40 (2005) 1615 – 1623,
30. Gibson, R. F. (1976). Dynamic mechanical behavior of fiber-reinforced composites: Measurement and analysis, J. Compos. Mater. 10: 325–341.
31. Tevet-Deree L., The Dynamic Response of Composite Materials with Viscoelastic Constituents, MsS Thesis, BGU, 2003
32. Debotton G., Tevet-Deree L., (2004) The response of a fiber-reinforced composite with a viscoelastic matrix phase, Journal of Composite Materials, Vol. 38, No. 14, 1255-1277
33. J. M. L. dos Reis, Mechanical characterization of fiber reinforced Polymer Concrete. Materials Research. 2005, vol.8, no.3, p.357-360

34. R. W. Venderbosch, T. Peijs, H. E. H. Meijer, P. L. Lemstra, Fibre-reinforced composites with tailored interphases using PPE/epoxy blends as a matrix system, Composites A, Applied science and manufacturing, 1996, vol. 27, no 9 (26 ref.), pp. 895-905
35. L. Mishnaevsky Jr, P. Brøndsted, Micromechanisms of damage in unidirectional fiber reinforced composites with ductile matrix: computational analysis, Presentation on 2nd International Conference on Recent Advances in Composite Materials (ICRACM - 2007), New Delhi, 20-23 March 2007 (in print)
36. Venkateswara Rao K. T. ; Siu S. C. ; Ritchie R. O. Failure mechanisms in SiC-fiber reinforced 6061 aluminum alloy composites under monotonic and cyclic loading 1993, Metallurgical transactions. A, vol. 24, no3, pp. 721-734
37. Feih, S.; Wonsyld, K.; Minzari, D.; Westermann, P.; Lilholt, H., Testing procedure for the single fiber fragmentation test. Risø-R-1483(EN) (2004) 30 p.